Critical Experiment and Depletion Benchmark Analyses with ENDF/B-VIII.1 Evaluated Nuclear Data Library

Jimin Hur [a] and Ho Jin Park [a*]

[a]*Kyung Hee Univerisity, 1732, Deogyeong-daero, Giheung-gu, Yongin-si, 17104, Korea*

[*]*Corresponding author: parkhj@khu.ac.kr*

***Keywords :** ENDF/B-VIII.1, McCARD, ICSBEP, VERA benchmark, Uncertainty Quantification

1. Introduction

In a regulation body for nuclear core design, it is recommended to perform core analysis using the up-to-date nuclear data libraries (ENDLs). The ENDF/B ENDL has been internationally used after released since the first version in the 1960s. ENDF/B-VII., ENDF/B-VII.1 and ENDF/B-VIII.0 has released in 2006, 2011, and 2018, respectively.

Recently, the newest version of ENDF/B, ENDF/B-VIII.1 was released on October 21, 2024 [1,2]. It contained updates to the neutrons, charged particles, fission yields sub-libraries. In the neutron sub-library, one of the most significant updates was the revision of the ^{239}Pu file, which has improved its accuracy and reliability by a joint international effort. Moreover, ^{233}U, ^{235}U, ^{238}U, ^{240}Pu, and ^{241}Pu neutron reaction cross sections were updated by the IAEA-coordinated INDEN collaboration. In the ENDF/B-VIII.1, a number of thermal scattering cross sections have been re-evaluated. In addition, new covariance testing has been implemented.

The goal of this study is to investigate the impact of the newly released ENDF/B-VIII.1 cross section and their uncertainties on criticality experiment benchmark problems and to compare the results with those obtained using the previous versions of ENDF/B (e.g., ENDF/B-VII.1, ENDF/B-VIII.0 [3]) through McCARD [4] Monte Carlo (MC) calculations.

2. Criticality Benchmark Analyses with ENDF/B-VIII.1

McCARD analyses of the selected International Criticality Safety Benchmark Problems (ICSBEP) [5] are performed with ENDF/B-VIII.0 and ENDF/B-VII.1 to compare them. The selected critical benchmark problems are divided into the four categories due to a type of fuel: plutonium (PU), high enriched uranium (HEU), low enriched uranium (LEU), and ^{233}U (U233). All McCARD calculations are conducted using the same neutron history condition: 100,000 neutron histories per cycle, 1000 active cycles, and 50 inactive cycles.

2.1 Plutonium Criticality Benchmark Analyses

Figure 1 compares the calculated to experimental (C/E) values of multiplication factors by McCARD code for PU benchmark suites. The root mean square (RMS) error between reference and McCARD are 349 pcm, 428 pcm, and 374 pcm, respectively. In the eight PU fast spectrum benchmarks, there are no large differences between ENDL files. On the other hand, the multiplication factor of ENDF/B-VIII.1 for PU thermal benchmark problem has risen back to a level similar to ENDF/B-VII.1.

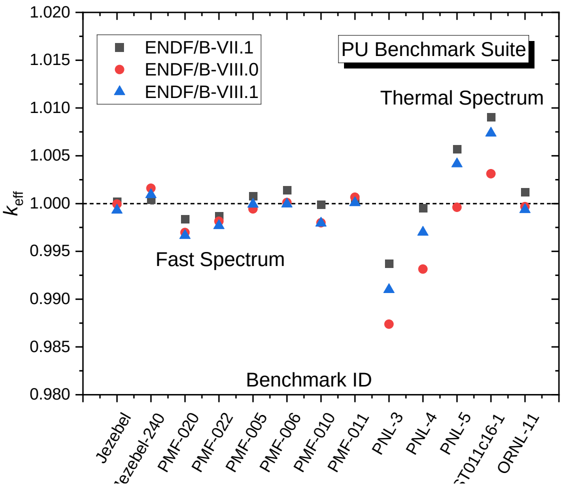

Fig. 1. Comparison of multiplication factors by McCARD for Plutonium ICSBEP benchmark problem.

In the previous update, ENDF/B-VIII.0 adopted a focused international effect on ^{239}Pu via CIELO project. It was known that “the neutron capture cross section on ^{239}Pu has been poorly known with uncertainty exceeding 10% in the fast region” [3]. Figures 2 and 3 show the ^{239}Pu capture and fission cross section for ENDF/B-VII.1, ENDF/B-VIII.0, and ENDF/B-VIII.1 in the PNL-5 PU thermal spectrum benchmark problem. It is noted that there are significant changes in the capture cross section for ENDL versions in the fast energy region and within the 0.1 eV to 10 eV range. Because the ^{239}Pu fission cross section shows no large differences between ENDL files, the multiplication factor of ENDF/B-VIII.1 leads to a value similar to that of ENDF/B-VII.1. The changes in ^{239}Pu cross sections across different ENDLs indicate uncertainties, which may be considered as the source of errors in the Pu thermal benchmark problems.

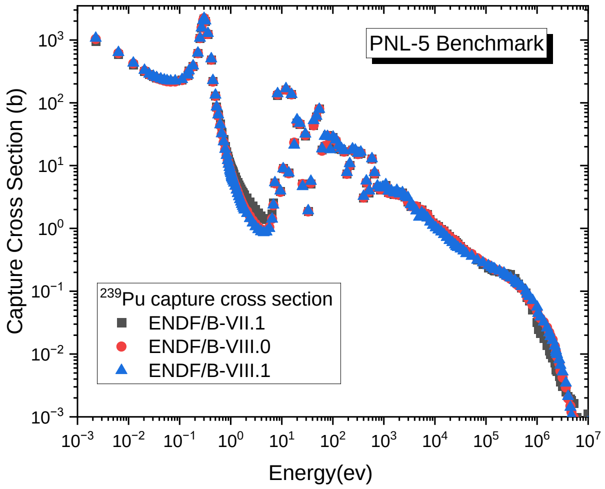

Fig. 2. ^{239}Pu multi-group capture cross section for ENDF/B-VII.1, ENDF/B-VIII.0, and ENDF/B-VIII.1 in PNL-5 PU thermal benchmark problem.

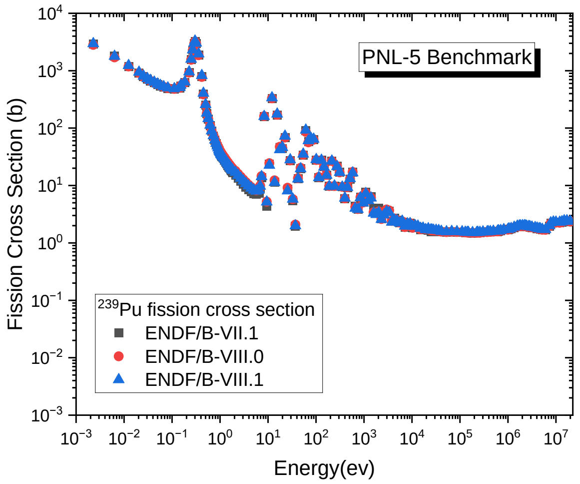

Fig. 3. ^{239}Pu multi-group fission cross section for ENDF/B-VII.1, ENDF/B-VIII.0, and ENDF/B-VIII.1 in PNL-5 PU thermal benchmark problem.

2.2 HEU Criticality Benchmark Analyses

Figure 4 shows the C/E multiplication factors by the McCARD code for HEU benchmark suites. The RMS errors between reference and C/E values are 310 pcm, 266 pcm, 236 pcm, respectively. Except for HMF-027 and the thermal benchmark problems (ORNL series), there is no significant difference between ENDF/B-VIII.0 and ENDF/B-VIII.1. The HMF-027 benchmark problem is the lead-reflected core of ^{235}U 90 w/o based on the VNIEF critical test facility. The ENDF/B-VIII.1 release group mentioned that significant change for Lead (i.e.,^{206}Pb-^{208}Pb) were included as a key advance [2]. Figure 5 compared with ^{208}Pb scattering cross section for each ENDL version. It is observed that the scattering cross-section in ENDF/B-VIII.1 has increased in the fast energy region compared to ENDF/B-VIII.0. In the HMF-027 problem, lead is used as the reflector material. Therefore, an increase in the ^{208}Pb scattering cross-section leads to an increase in multiplication factors.

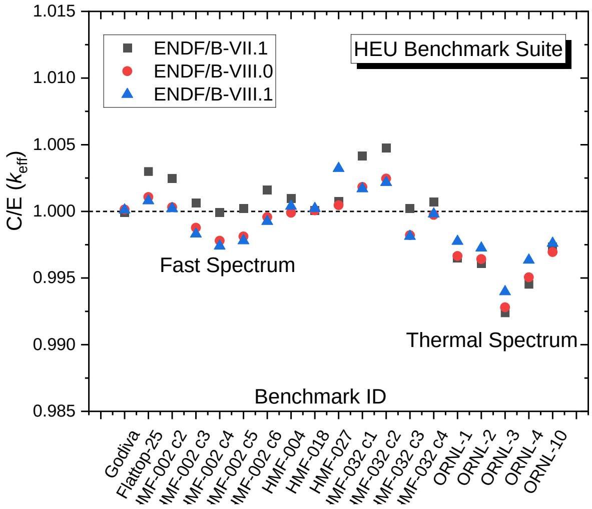

Fig. 4. Comparison of multiplication factors by McCARD for High Enriched Uranium ICSBEP benchmark problem.

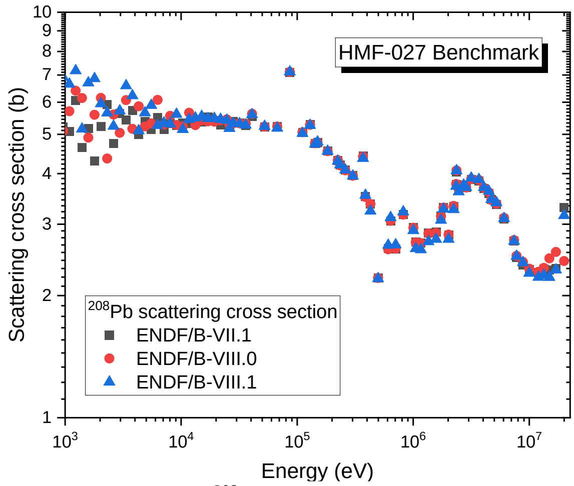

Fig. 5. Comparison of ^{208}Pb scattering cross sections for HMF-027 HEU fast benchmark problem.

2.3 LEU Criticality Benchmark Analyses

Figure 6 compared the C/E values of the multiplication factors by the McCARD code for LEU benchmark suites. In the LEU benchmark cases, there is no significant difference in the multiplication factor among three ENDLs. The RMS errors between reference and C/E values for ENDF/B-VII.1, ENDF/B-VIII.0, and ENDF/B-VIII.1 are 124 pcm, 109 pcm, 111 pcm, respectively. Interestingly, in the case of the LCT-010 problems, there is a noticeable difference between ENDF/B-VIII.0 and ENDF/B-VIII.1. The LCT-010 case 9 to case 19 consists of water-reflected fuel pin clusters with reflecting walls made of steel. Figure 7 shows the change of ^{56}Fe absorption cross section for LCT-010 benchmark problem. The decreases of ^{56}Fe absorption cross section can lead to the increases in multiplication factors as shown in Fig. 6.

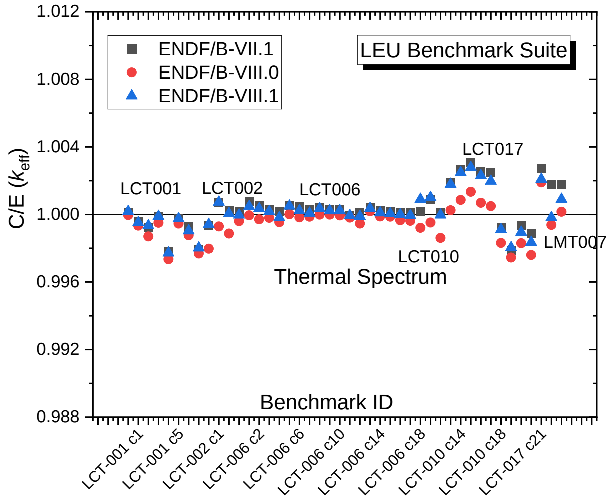

Fig. 6. Comparison of multiplication factors by McCARD for Low Enriched Uranium ICSBEP benchmark problem.

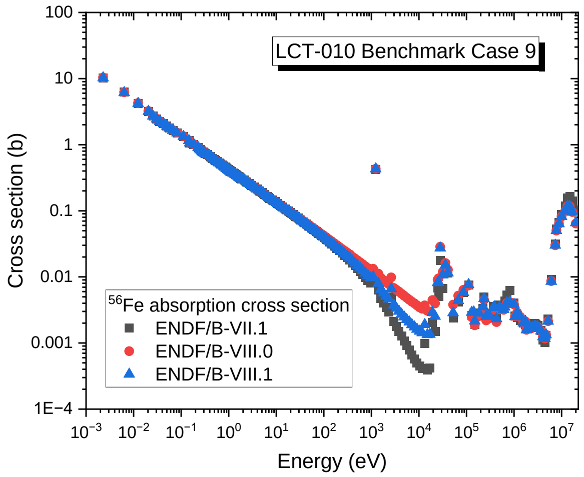

Fig. 7. Comparison of ^{56}Fe absorption cross sections for LCT-010 LEU thermal benchmark problem.

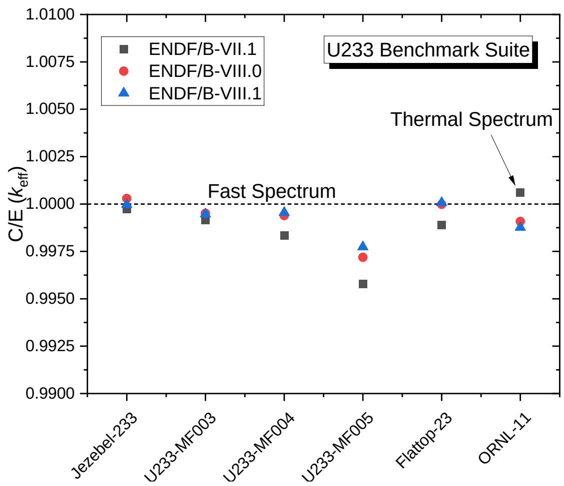

Fig. 8. Comparison of multiplication factors for U233 ICSBEP benchmark problem.

2.4 U233 Criticality Benchmark Analyses

Figure 8 compared the C/E values of the multiplication factors by the McCARD code for U233 benchmark suites. The RMS errors between reference and C/E values for ENDF/B-VII.1, ENDF/B-VIII.0, and ENDF/B-VIII.1 are 196 pcm, 126 pcm, 109 pcm, respectively. There are no significant differences in multiplication factors among three ENDLs. It should be noted that the number of U-233 benchmark cases considered in this study is small. Table I summarized the RMS errors of multiplication factors for each ICSBEP category. The total number of the ICSBEP problems for ENDF/B-VIII.1 benchmarking is 85.

Table I: RMS errors of multiplication factors for each ICSBEP category

Category (# of problems)	RMS errors of multiplication factors (pcm)		
	ENDF/B-VII.1	ENDF/B-VIII.0	ENDF/B-VIII.1
PU (13)	349	428	374
HEU (28)	310	266	236
LEU (43)	124	109	111
U233 (6)	196	126	109
Total (85)	249	238	216

* statistical uncertainties are less than 30 pcm.

3. Depletion Benchmark Analyses with ENDF/B-VIII.1

3.1 VERA depletion benchmark problem

To examine the effect of ENDF/B-VIII.1 ENDL for burnup analyses, VERA depletion benchmark [6] analyses was conducted by the McCARD MC code. The problems 1C and 2C were selected among the VERA depletion benchmark problems. In this study, all burnup analyses were conducted from a constant extrapolation at the predictor stage and a backward extrapolation at the corrector stage (CEBE) by matrix exponential method depletion equation solver with 10 sub-steps (MEMSUB) [7]. At each depletion time step (DTS), all McCARD calculations are conducted using the same neutron history condition: 10,000 neutron histories per cycle, 500 active cycles, and 50 inactive cycles. Under this condition, the maximum statistical uncertainty of multiplication factor is less than 30 pcm.

3.2 ENDF/B-VIII.1 benchmarking for VERA depletion problem

Figure 9 compares k_{inf}'s over burnup for each ENDL in VERA benchmark problem 1C. It was already known that previous studies [8] have shown that in ENDF/B-VIII.0, the multiplication factor tends to be underestimated over burnup compared to ENDF/B-VII.1.

As shown in Table II, the RMS difference between ENDF/B-VII.1 and ENDF/B-VIII.0 was 208 pcm, while ENDF/B-VIII.1 reduced this difference to 111 pcm. At end of cycle (EOC), the k_{inf} in ENDF/B-VIII.1 appears closer to that of ENDF/B-VII.1.

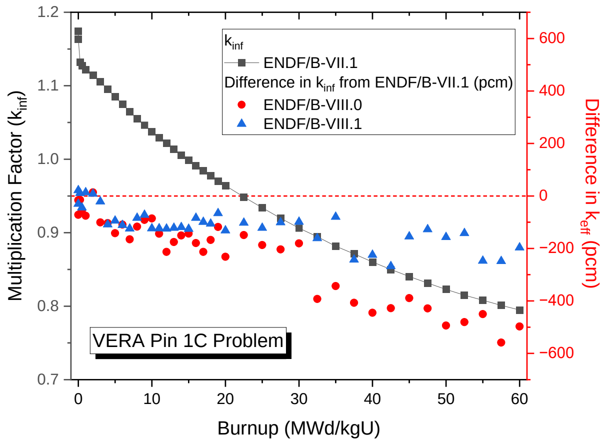

Fig. 9. Comparison of k_{inf} by McCARD burnup analyses for each evaluated nuclear data library in problem 1C.

Table II: RMS errors and k_{inf} at EOC (60MWd/kgU) for problem 1C with varying the number of depletion time steps.

Case	RMS errors (pcm)	k_{inf} (EOC)
ENDF/B-VIII.0	208	0.79177
ENDF/B-VIII.1	111	0.79366
ENDF/B-VII.1		0.79490

* statistical uncertainties are less than 30 pcm.

Figure 10 compares ^{235}U one-group (n,g) cross section over burnup for each ENDL in problem 1C. The increases in ^{235}U one-group cross section can lead to the decrease in ^{235}U number density. Ultimately, the reduction in ^{235}U leads to a decrease in the multiplication factor as shown in Fig. 9.

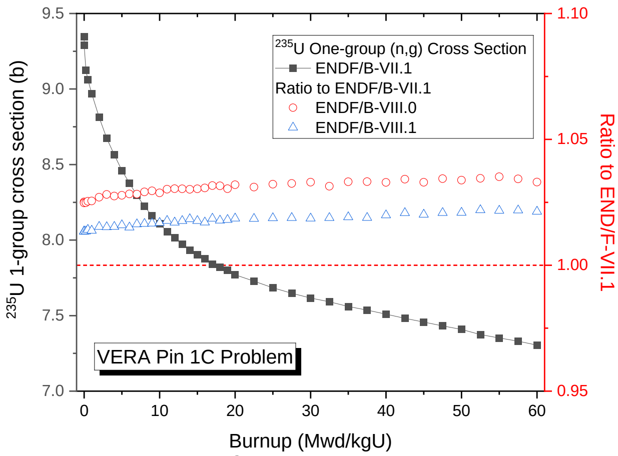

Fig. 10. Comparison of ^{235}U one-group (n,g) cross sections over burnup for each ENDL in problem 1C.

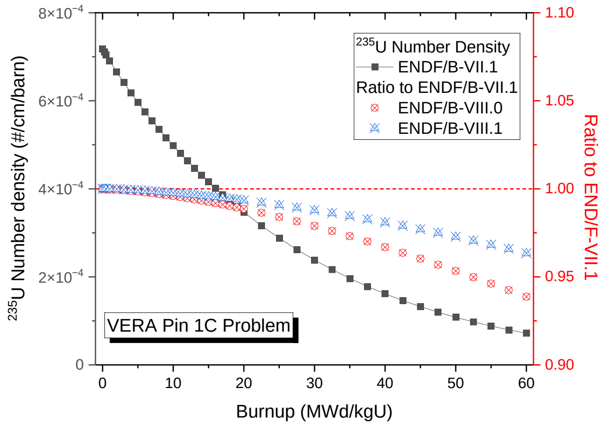

Fig. 11. Comparison of ^{235}U number densities over burnup for each ENDL in problem 1C.

Figure 12 plots k_{inf} by McCARD calculations with the three ENDLs over burnup. The RMS differences in k_{inf} between ENDF/B-VII.1 and the other two ENDLs are 238 pcm and 129 pcm, respectively.

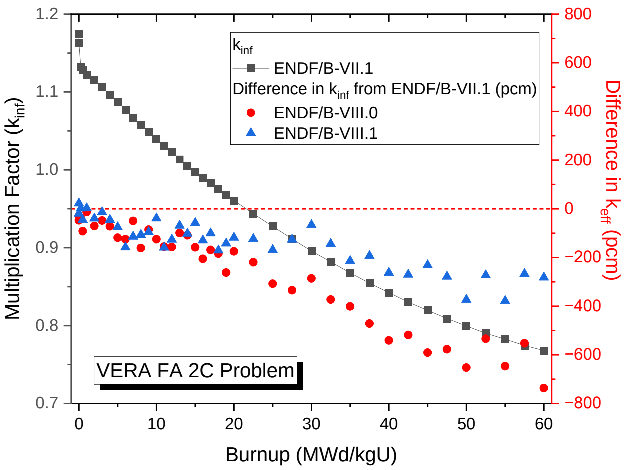

Fig. 12. Comparison of k_{inf} by McCARD burnup analyses for each evaluated nuclear data library in problem 2C.

4. Uncertainty Quantification in Multiplication Factors with ENDF/B-VIII.1

4.1 Uncertainty quantification in multiplication factors by McCARD code

The ENDF/B-VIII.1 release group mentioned that new covariance data was provided in the ENDF/B-VIII.1 version [2]. The McCARD code has a capability to perform sensitivity and uncertainty (S/U) analyses using the Seoul National University (SNU) S/U formulation. This SNU S/U formulation can be used to quantify the uncertainty of multiplication factor k. It can consider both statistical uncertainty and the uncertainty arising from MC input data variations. The uncertainty of multiplication factor k due to uncertainties of nuclear cross section input data can be quantified by

$$\sigma_{xx}^2(k) \cong \sum_{i,\alpha,g}\sum_{i',\alpha',g'} \mathrm{cov}[x_{\alpha,g}^{i}, x_{\alpha',g'}^{i'}]\left(\frac{\partial k}{\partial x_{\alpha,g}^{i}}\right)\left(\frac{\partial k}{\partial x_{\alpha',g'}^{i'}}\right) \quad (1).$$

where $x_{\alpha,g}^{i}$ is the α -type cross section of nuclide i for energy group g and $\mathrm{cov}[x_{\alpha,g}^{i}, x_{\alpha',g'}^{i'}]$ is the covariance matrix between them. The NJOY code can generate multigroup covariance matrices using the evaluated nuclear data library. The sensitivity coefficients in Eq. (1) can be calculated by the MC perturbation technique or the adjoint flux weighted perturbation (AWP) method [9].

4.2 Uncertainty quantification in multiplication factors for Godiva and Jezebel benchmarks

In the Godiva problem, for uncertainty quantification (UQ) analyses, 30 group covariance matrices of ^{235}U and ^{238}U nuclear cross sections are generated and analyzed through the McCARD S/U formulation. Table III displays the contribution of ^{235}U and ^{238}U nuclear cross sections to uncertainties of the multiplication factor in the Godiva problem. Uncertainties from minor effective covariance data (e.g., covariance data between (n,2n) and (n,3n)) are also included in total uncertainty for each library. The most significant contributor of ENDF/B-VIII.I and ENDF/B-VIII.0 was ^{235}U fission cross section (MT=18), unlike the one of ENDF/B-VII.1, which was ^{235}U gamma cross section (MT=102). It should be noted that the uncertainties of the multiplication factors show no significant difference between ENDF/B-VIII.0 and ENDF/B-VIII.1, suggesting that there have been no noticeable updates in the ^{235}U and ^{238}U covariance data between the two libraries. Figure 15 presents a comparison of ^{235}U cross section uncertainties between three ENDLs. In fission cross section, for example, it is noted that ENDF/B-VIII.I and ENDF/B-VIII.0 show high agreement in the whole energy region. This leads to similar uncertainties for ENDF/B-VIII.I and ENDF/B-VIII.0.

In the Jezebel problem, covariance data for ^{239}Pu, ^{240}Pu and ^{241}Pu were considered in the S/U analyses. Table III also displays the contribution of ^{239}Pu and ^{240}Pu nuclear cross sections to uncertainties of the multiplication factor in the Jezebel problem. Given that ^{239}Pu is the predominant isotope in the Jezebel problem, it is observed that the uncertainties associated with the other two nuclides have a negligible effect. There is no significant difference in the multiplication factor from ^{240}Pu and ^{241}Pu between the three ENDLs, indicating that there have been no marked changes in the covariance data across there ENDLs.

Conversely, the covariance data for ^{239}Pu has undergone a notable change. The three largest contributors for ENDF/B-VII.1 and ENDF/B-VIII.0 are inelastic scattering (MT=4), fission (MT=18), and elastic scattering (MT=2). The update from ENDF/B-VIII.0 to ENDF/B-VIII.1 resulted in a modest decrease in the uncertainty by the three contributors. The ν (MT=452) covariance of ^{239}Pu shows a tendency for increasing uncertainty impact as the ENDL is updated (from 0.081% to 0.414%).

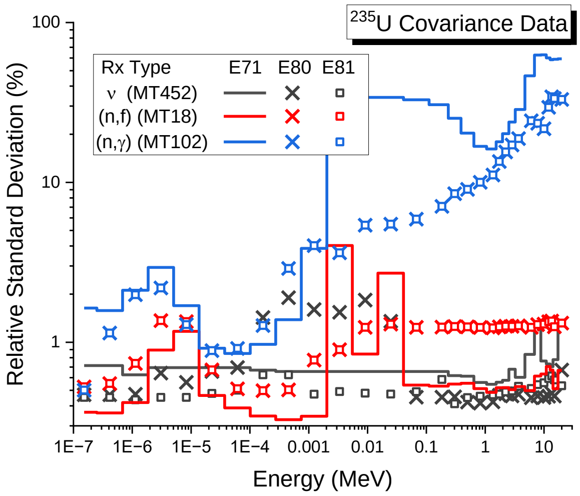

Fig. 15. Comparison of the ^{235}U cross section uncertainties among ENDF/B-VII.1 (E71), ENDF/B-VIII.0 (E80), and ENDF/B-VIII.1 (E81).

Table III: Uncertainties of multiplication factors in Godiva and Jezebel benchmark problem due to the nuclear cross section data uncertainties, $\sigma_{xx}(k)$ [%]

Covariance Data	Godiva				Jezebel			
	Nuclide	ENDF/B-VII.1	ENDF/B-VIII.0	ENDF/B-VIII.1	Nuclide	ENDF/B-VII.1	ENDF/B-VIII.0	ENDF/B-VIII.1
ν , ν	^{235}U	0.542	0.398	0.389	^{239}Pu	0.081	0.316	0.414
(n,γ) , (n,γ)		0.877	0.284	0.285		0.074	0.076	0.023
(n,fis) , (n,fis)		0.266	0.778	0.777		0.328	0.896	0.535
(n,n) , (n,n)		0.286	0.282	0.278		0.451	0.480	0.375
(n,n') , (n,n')		0.570	0.212	0.213		0.794	0.820	0.637
ν , ν	^{238}U	0.011	0.011	0.011	^{240}Pu	0.008	0.008	0.008
(n,γ) , (n,γ)		0.001	0.003	0.003		0.017	0.017	0.017
(n,fis) , (n,fis)		0.003	0.008	0.008		0.012	0.013	0.013
(n,n) , (n,n)		0.027	0.015	0.016		0.031	0.028	0.031
(n,n') , (n,n')		0.072	0.023	0.023		0.054	0.052	0.055
Total		1.178	1.012	0.998	Total	0.519	1.270	0.739

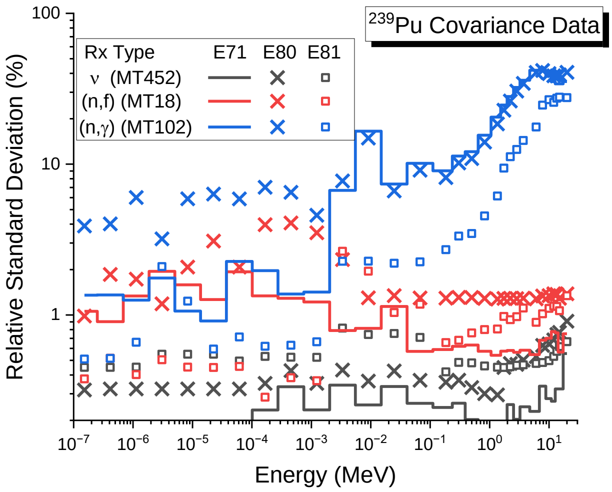

Fig. 16. Comparison of the ^{239}Pu cross section uncertainties among ENDF/B-VII.1 (E71), ENDF/B-VIII.0 (E80), and ENDF/B-VIII.1 (E81).

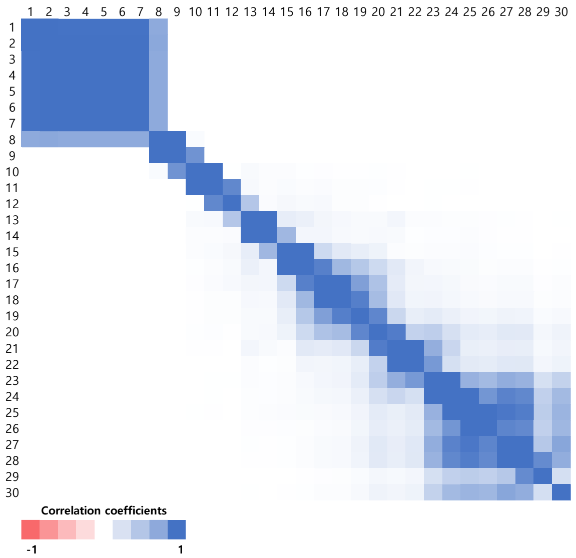

Fig. 17. Correlation coefficient matrix of ^{239}Pu ν (MT=452) for ENDF/B-VII.1.

Figure 16 presents a comparison of ^{239}Pu cross section uncertainties between three ENDLs. Uncertainties of the fission and capture cross sections for ENDF/B-VIII.1 are mostly smaller than those for ENDF/B-VIII.0 in the fast energy region. It leads to a reduction in the uncertainty of the multiplication factor for ENDF/B-VIII.0 compared to ENDF/B-VIII.1.

Uncertainty from the number of neutrons per fission (ν) raised from ENDF/B-VII.I to ENDF/B-VIII.0, and ENDF/B-VIII.1, which is also based on differences in covariance data. Figures 17–19 present correlation matrix of ν of ^{239}Pu for ENDF/B-VII.I, ENDF/B-VIII.0, and ENDF/B-VIII.1, respectively. Note that only ^{239}Pu was calculated with the ν value as MT=452. Meanwhile, covariance data of ν is only given for MT=456, which represents an average number of prompt neutrons per fission, for ^{240}Pu and ^{241}Pu. Significant changes are observed in the correlation coefficient matrix. The correlation matrix provided in ENDF/B-VII.1 takes the form of a diagonal matrix. The thermal and fast cross sections in ENDF/B-VIII.0 and ENDF/B-VIII.1 are grouped separately and show strong positive correlations within each group. These correlations can potentially enhance the increase of uncertainty to the multiplication factor.

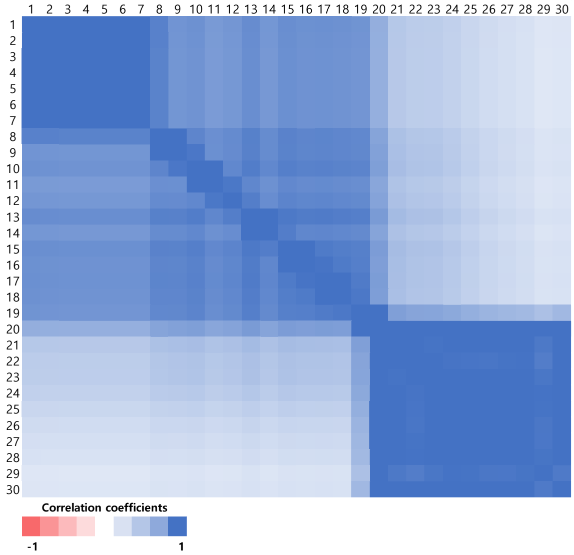

Fig. 18. Correlation coefficient matrix of ^{239}Pu ν (MT=452) for ENDF/B-VIII.0.

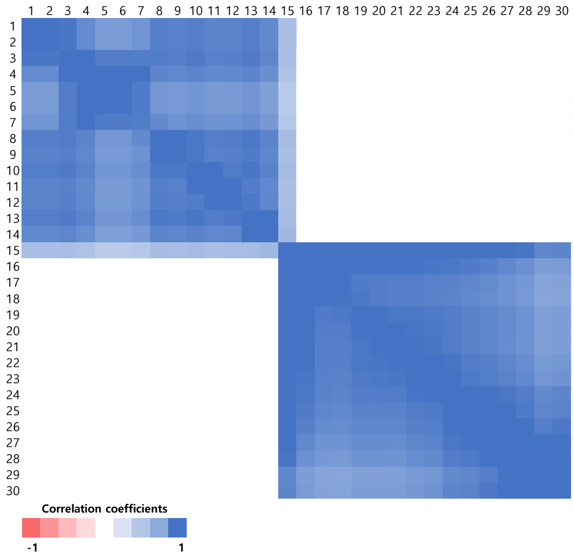

Fig. 19. Correlation coefficient matrix of ^{239}Pu ν (MT=452) for ENDF/B-VIII.I.

5. Conclusions

In this study, the impact of the newly released ENDF/B-VIII.1 cross-section data and its uncertainties on criticality experiment benchmark problems were assessed using the McCARD code. The results are compared with those from the previous ENDF/B versions: ENDF/B-VII.1 and ENDF/B-VIII.0. The changes in multiplication factors by the re-evaluation of

^{239}Pu by a joint international effort and the changes for lead, uranium, and cooper were confirmed in the ICSBEP benchmark analyses. Moreover, it was noted that the reduction in the multiplication factor at EOC in ENDF/B-VIII.1 is mitigated compared to that in ENDF/B-VIII.0. The uncertainties in multiplication factors for representative S/U benchmark problems due to the covariance data updated in ENDF/B-VIII.1 were confirmed.

In the near future, we will examine the reduced bias in ENDF/B-VIII.1 in various criticality benchmarks experiments containing fluorine, copper, and stainless steel. Moreover, we plan to assess the impact on commercial light water reactors and Gen-VI reactors using ENDF/B-VIII.1.

Acknowledgement

This paper is a result of The Human Resources Development Project for HLW Management hosted by KORAD and MOTIE.

REFERENCES

[1] Gustavo Nobre1, David Brown, Ramon Arcilla, Rebecca Coles, and Benjamin Shu, Progress towards the ENDF/B-VIII.1 release, EPJ Web of Conferences 294, 04004, 2024.
[2] https://www.nndc.bnl.gov/endf-library/B-VIII.1/
[3] D.A. Brown et al, ENDF/B-VIII.0: The 8th Major Release of the Nuclear Reaction Data Library with CIELO-project Cross Sections, New Standards and Thermal Scattering Data, Nuclear Data Sheets, Vol 148, p 1-142, 2018.
[4] H. J. Shim et al., McCARD: Monte Carlo Code for Advanced Reactor Design and Analysis, *Nucl. Eng. Technol.*, Vol. 44, p 161-176, 2012.
[5] "International Handbook of Evaluated Criticality Safety Benchmark Experiments," OECD Nuclear Energy Agency report NEA/NSC/COD(95)03, 1998 Edition.
[6] K.S. Kim, "Specifications for the VERA Depletion Benchmark Suite," CASL-U-2015-PHI.VCS.P11.02-010, Oak Ridge National Laboratory, 2015.
[7] H. J. Park et al., Monte Carlo burnup and its uncertainty propagation analyses for VERA depletion benchmarks by McCARD, *Nucl. Eng. Technol.*, Vol. 50, pp. 1043-1050, 2018.
[8] H. J. Park et al., Comparison of ENDF/B-VIII.0 and ENDF/B-VII.1 in criticality, depletion benchmark, and uncertainty analyses by McCARD, *Ann. Nucl. Energy*, Vol. 131, pp. 443–459, 2019.
[9] H. J. Shim and C. H. Kim, Adjoint Sensitivity and Uncertainty Analyses in Monte Carlo Forward Calculations, *J. Nucl. Sci. Technol.*, Vol.48, p.1453-1461, 2011.